FEM Simulations of ISO 14801 Implant Fatigue Test Setup

A. Eser, T. Albrecht, S. Heintze

R&D, Ivoclar Vivadent AG, Bendererstrasse 2, FL-9494 Schaan, Liechtenstein

***Abstract**: To replace missing teeth with dental implants is a common and clinically proven treatment option. However, there are still several complications with this kind of treatment. Besides biological complications like periimplantitis, the most common technical complication is loosening or fracture of the screw which is mainly due to fatigue. The purpose of this investigation is to appraise a ranking of the fatigue behavior of six different implant systems by finite element method (FEM) simulations in order to figure out the "worst case" implant system for the fatigue testing according to ISO standard 14801. The simulations were conducted according to the guidance of the US Food and Drug Association (FDA) "Reporting of Computational Modeling Studies in Medical Device Submissions". Nonlinear FEM simulations were conducted by Abaqus/Standard by taking into account the contact condition between implant, abutment and screw. Simulation results showed a good correlation with the experimental findings. Not only could the exact position of the fracture be reproduced but also could an exact ranking of the implant systems due to the level of the fracture force be realized by the FEM simulations.*

***Keywords**: Implantable Medical Device, Bolt Loading, Experimental Verification, Failure, Fatigue*

1. Introduction

The clinical insertions of dental implants to replace missing teeth have grown over the last 20 years very rapidly in industrialized countries. In 2015 about 15 million implants had been placed worldwide with 34% in Europe, 22% in Latin America, 20% in Asia, and 18% in North America [1]. The main indications are the replacement of single teeth. In 2015 about two thirds of all implants had been placed in conjunction with crowns and bridges and about one third to retain dentures [1]. Although most of the clinical studies reported higher success rates for dental implants, several complications are still frequently observed. The most frequent complications are bone loss and eventually loss of the implant, screw loosening/fracture, veneer chipping, fracture of the framework and fracture of the implant itself [2-5].

The major reason associated with the technical complications for dental implants is known to be due to mechanical fatigue as the implants are subjected to repeated masticatory load in the oral environment throughout the whole service life [6-8]. Therefore, in 2003 a standardized fatigue testing protocol was introduced by the International Organization for Standardization (ISO 14801:2003) and subsequently revised in 2007 and 2016. According to this standard, the testing should be conducted at 2 Hz and carried and 2.10^6 in liquid media or conducted at 15 Hz and 5.10^6 cycles in dry conditions [9]. At least two specimens should be tested at four loading levels and three specimens should survive without failure at a given load level (2.10^6 in liquid media, 5.10^6 in air). In this procedure, the implant is to be tested under "worst case" conditions which include tilting the implant by a certain angle, usually 30° with respect to its longitudinal axis, in order to induce bending stresses that are representative of the implant's inclination in the oral cavity. An alternative procedure the so-called "stair case method" was introduced in the revision of 2017, which can decrease the testing time and number of specimens. However, fatigue testing of implant systems due to ISO 14801 is still very costly due to long testing time with expensive test equipment, specimen preparation and the material itself. At this point, the usage of the finite element method (FEM) simulations can be helpful to replace some of these physical testing procedures.

For dental implants, FEM simulations have been widely used to evaluate the mechanical performance [10-15]. Most of the existing simulations in the literature were conducted to evaluate the stress conditions under static loading. Furthermore there are several studies which combine FEM simulations with fatigue analysis [16-22].

In 2014 the FDA released a guidance document on "Reporting of Computational Modeling Studies in Medical Device Submissions" which was revised in 2016 [23]. The guidance not only gives recommendations how to report the simulation results but also gives some hints on how to verify and validate the simulation results.

The objective of this study is to simulate six different implant systems to figure out the "worst case" implant system which correspond to the one with the lowest maximum endured load and the lowest fatigue limit. The simulations and the corresponding experiments are planned to be used as a verification of the simulation model developed in this study. This verified simulation model can be used in the future for FDA submissions to replace experiments with FEM simulations. For the first prediction, the maximum principal stress (σ_{max}) values were used to rank the fatigue performance of the investigated implant systems. Not only a good correlation between the location of the maximum values of σ_{max} observed from the simulation results but also the ranking of the maximum values of σ_{max} can be very good validated from the experimental findings.

2. Materials and Methods

2.1 Mechanical Testing

Dynamic fatigue testing of 6 different implant systems (Table 1) was conducted according to ISO 14801:2007. A finished specimen consisted of a titanium implant, and an IPS e.max CAD abutment crown (Ivoclar Vivadent, Liechtenstein) adhesively luted to a Sirona titanium base (TiBase). The abutment or hybrid crown is not an anatomically shaped crown rather a coping type of crown adapted to the test set-up. In Table 1 in the column "Implant System" the abbreviations of the implant systems are given which are used for the corresponding systems in this report. All dynamic tests were performed at the Fraunhofer Institute for Mechanics of Materials (IWM) in Freiburg/Germany.

Table 1. Implant systems

Implant System					Stock abutment Sirona TiBase		
Supplier	**System/Type**	**Abbreviation**	**Ref**	**∅ [mm]**	**Type**	**Ref.**	**Size**
Straumann	Standard Tissue Level RN	**Stmn TL**	043.253S	4.8	S SO 4.8 L	6284249	L
Dentsply-Sirona	Friadent XiVE S	**Friad XIVE**	26-2435	3.4	TiBase FX 3.4 S	6282433	S
Nobel Biocare	Replace TG NP	**NB Replace**	32214	3.5	TiBase NB RS 3.5 L	6282474	L
	Brånemark System Mk III TiU NP	**NB Branemark**	28909	3.3	TiBase NB B 3.4 L	6282516	L
Biomet 3i	Biomet 3i OSSEOTITE	**Biomet OSSEO**	OSM 318	3.25	TiBase B O 3.4 L	6282557	L
Zimmer	TSV with MTX	**Zimmer TSV**	TSVB16	3.50	TiBase Z TSV 3.5 L	6282581	L

Figure 1 shows the technical design of the entire test set-up with embedded implant in specimen holder, titanium abutment (TiBase), screw, angled abutment crown, hemisphere and pendulum. All dimensions meet the minimal requirements given in the instructions for use of IPS e.max CAD abutment solutions.

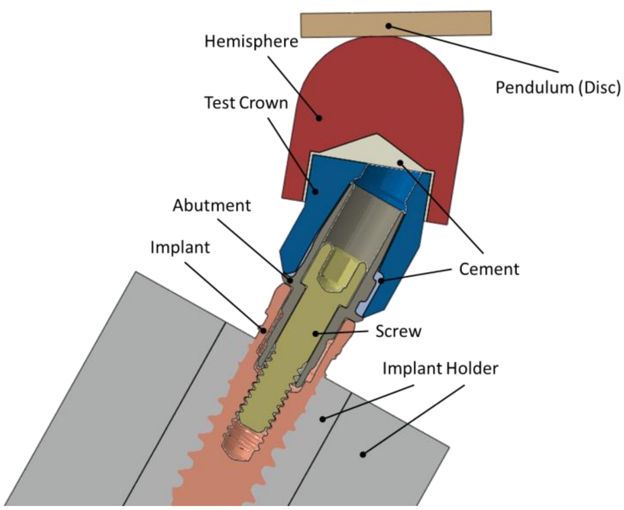

Figure 1. Technical design of the experimental test setup according to ISO 14801.

To simulate a worst case scenario the implant’s long axis was mounted at a 30° angle in the loading direction in combination with a 20° abutment crown angulation. Design and ceramic thickness are designed to fulfill the minimum requirements as recommended in the instructions for use of the hybrid abutment. The pretreatment, connection and luting were performed as described in the instruction for use.

The abutment screws were tightened with the torque values recommended by the manufacturers. The composite resin based luting material Multilink Hybrid Abutment HO0 (Ref. 647182AN, Lot. R68920) was used to lute the ceramic meso-structure crown onto the titanium base. The pretreatment, connection and luting were performed as described in the instruction for use. The specimens were sterilized by steam sterilization (Vacuklav® 40-B, Melag) in an autoclave at 134 °C for 3:30 minutes.

A brass specimen holder with 7mm diameter was used for the testing. The loading was conducted with servohydraulic/electric testing machines (MTS 858 MiniBionix II, MTS Systems; MiniBionix Test System, MTS Systems, custom-made servo-hydraulic testing machine with MTS control unit "FlexTest SE", IWM-Fraunhofer; custom-made servo-hydraulic testing machines with validated Fraunhofer IWM control and measuring system, IWM-Fraunhofer,; electrodynamic testing machines: DORA 14801, Larado Medizintechnik) with a 2 Hz sinusoidal pulsating load. The load was transferred by a steel bar of 100mm length, fixed to the machine piston by a flexible joint, thus avoiding transverse forces.

The implants were loaded at different force levels. After dynamic loading the specimens were examined for damage with a stereo microscope (Leica M125, 20 x magnification). Testing started at higher load levels and the force level was dropped until three specimens survived after 2.10^6 cycles. This force level is defined as maximum endured load. The maximum endured load for the implant systems are presented in Table 2. Furthermore the fatigue (endurance) limit for each implant system was calculated with linear regression method (Table 2).

Table 2. Maximum endured load for the implant systems and the type of failure

	Friad XIVE	**Biomet OSSEO**	**NB Branemark**	**NB Replace**	**Zimmer TSV**	**Stmn TL**
Maximum Endured Load [N]	180	200	210	220	280	480
Fatigue Limit [N]	203	213	220	227	306	518
Minimum fracture Load [N]	200	240	250	280	320	600
Fracture Location	Fracture of screw	Fracture of implant	Fracture of Implant	Fracture of Implant	Fracture of Implant	Fracture of Implant

The type and the location the fracture were all reproducible for different implant systems. The location of the fracture will be discussed in the result chapter in comparison with the simulation results.

2.2 Finite Element Modelling

In order to simulate the entire test setup including the detailed geometry of the implant, screw and abutment, scans of these components were carried out with a micro X-Ray CT (VX8011-II PCB flex at Viscom AG, Hannover/Germany). Accordingly, a small uncertainty about the dimensions of those components may arise. It should here be emphasized that the average resolution of the scans which were carried out in this investigation was about 16µm. The raw scan data were converted to CAD data with the Cimatron E 12.0 software (3D Systems Software GmbH, Ettlingen/Germany).

The loading of the pendulum was applied on the upper node of the loading hemisphere. The loading force was set at 180 N which is the minimum of the maximum endured load from the tested implant systems (Friadent XiVE). The loading was applied with a 30° angulation to the implant's long axis (z-axis, Figure 2). Furthermore, the implant holder was assumed to be fixed on the outer boundaries of the cylinder (Figure 2). In order to verify the location of the fracture observed in the experiments with the simulations, further simulations were conducted with the fracture force from Table 2.

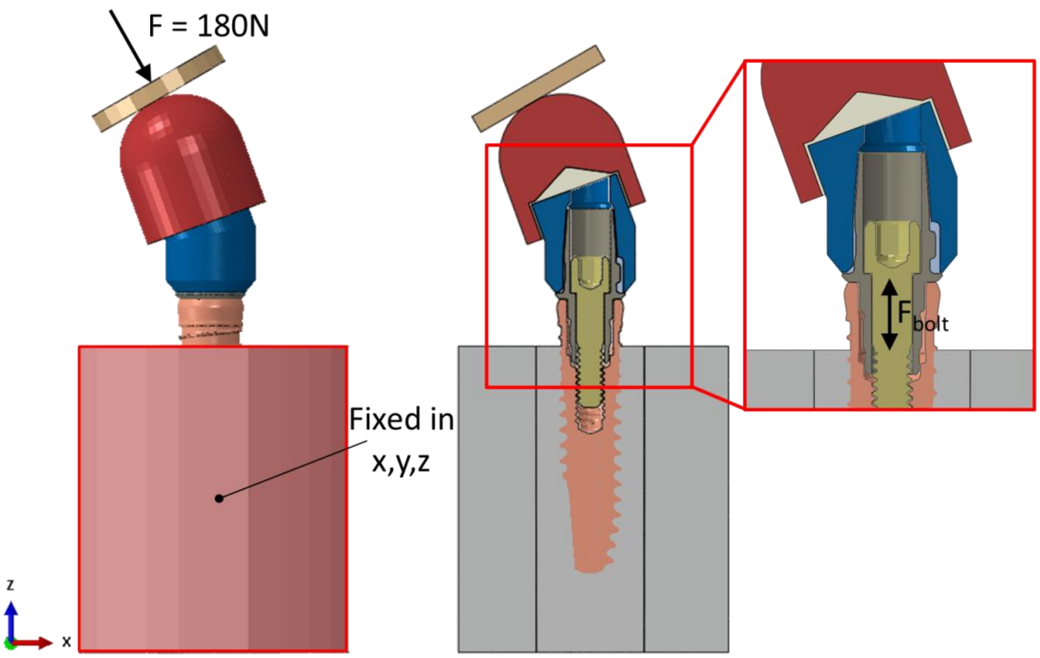

Figure 2. Boundary conditions and loading of the Friad XIVE implant system.

The screwing due to the applied torque is simplified by a bolt load in the axial direction. The torque values were achieved as an average value from the previous experiments to consider the loosing of the screw during dynamic loading. The axial clamping force (bolt load) was calculated from the following equation (Equation 1).

$$T = c.D.F_{bolt} \quad \text{(Equation 1)}$$

T is the average torque to loosen the screw after 2.10^6 cycles. c is the friction coefficient (0.3) and F is the bolt load force used in this study. The average torque values and the corresponding bolt loads are presented in Table 3.

Table 3. Average measured torque values to loosen the screw after 2.10^6 cycles and the corresponding bolt load calculated by Equation 1.

	Friadent XiVE	**Biomet OSSEO**	**NB Branemark**	**NB Replace**	**Zimmer TSV**	**Stmn TL**
T [Nmm]	70	85	85	85	115	200
F_{bolt} [N]	150	144	160	160	223	330

For the straightforwardness of the FEA, contact conditions between the components were assumed to be tied (Keyword: *Tie in Abaqus) expect for the components pendulum (disc)-hemisphere, abutment-screw, abutment-implant, and screw-implant. The contact definition was implemented with the general contact option in Abaqus (Keyword: *Contact Inclusions, ALL EXTERIOR). Contact properties were defined to be hard contacts with a friction coefficient of 0.3 using the penalty formulation (*Friction, slip tolerance=0.005, 0.3 and *Surface Behavior, pressure-overclosure=HARD).

Tetrahedral elements were used for the meshing of the complete model. The components hemisphere, disc, test crown and cement layers were meshed with 1^{st} order elements (C3D4 in Abaqus). The implant holders were separated into two parts. The part which was embedded in implant was meshed with 2^{nd} order elements (C3D10M) and the second part (outer part) with 1^{st} order elements. The other components namely implant, abutment and screw were all meshed with 2^{nd} order elements (C3D10M). A mesh convergence study with all elements meshed with 2^{nd} order elements showed that the effect of using 1^{st} order elements was negligible. The stress calculated in the components which are responsible for the failure of the specimens namely screw, abutment and implant did not significantly change with the model with only 2^{nd} order elements. Furthermore, a mesh convergence study was conducted to ensure that the element size was small enough to have a converged solution. Number of elements and nodes for the models used in this study are presented in Table 4. Meshing was done with the program Hypermesh v13.0 (Altair Engineering). Due to the complicated geometry, there were still distorted elements. However, the numbers of distorted elements (due to the criteria of Abaqus/Standard) for the models were only about 0.01 % of the total element number (for example 126 for the model FRIAD XIVE).

Table 4. Total numbers of elements/nodes for 6 implant systems

Implant System	Element Number	Node Number
Friad XIVE	679348	1559607
Biomet OSSEO	620049	1297675
NB Branemark	581457	1206586
NB Replace	577105	1213778
Zimmer TSV	584822	1198697
Stmn TL	545846	1143724

In order to save computation time, the materials are all assumed linear elastic stress-strain relationship was assumed to be linear elastic for all the materials. The constitutive equation for the linear elastic material behavior is as follows:

$$\boldsymbol{\sigma} = \mathbf{D}^{\mathbf{el}}\boldsymbol{\varepsilon}^{\mathbf{el}} \text{ (Equation 2)}$$

where $\boldsymbol{\sigma}$ is the Cauchy stress, $\boldsymbol{D}^{el}$ the fourth-order elasticity tensor and $\boldsymbol{\varepsilon}^{el}$ the total elastic strain.

The material properties used for this study are listed in Table 5.

Table 5. Material parameters used in this investigation

	Steel (disc/pendulum)	Multilink Automix (Adhesive cement)	Brass (cylinder)	e.max CAD (test crown)	CoCr (hemi-sphere)	Titanium (implant, abutment, screw)
Modulus of Elasticity [GPa]	210[24]	5.8 [24]	105 [25]	9.5 [26]	200 [24]	110 [24]
Poisson`s Ratio [-]	0.3[24]	0.23 [24]	0.346[25]	0.23 [26]	0.3 [24]	0.36 [24]

The simulations were conducted by using Abaqus/Standard (Dassault Systèmes). Nonlinear FEM simulations were conducted by taking into account the nonlinear displacement option which should deliver better results for the contact simulations.

3. Results

The simulated maximum stress values are presented in Table 6. The stress values in the table were reported from the nodes.

Table 6. Maximum value of the Von Mises stresses (σ_{VM}) and maximum principal stresses (σ_{max}), max endured load, and the location of the failure for the external load of 180N.

	IMPLANT		ABUTMENT		SCREW		Max. Endured Load [N]	Location of the failure
	σ_{max}	σ_{VM}	σ_{max}	σ_{VM}	σ_{max}	σ_{VM}		
Friad XIVE	373	713	190	386	732	571	180	Fracture of screw
Biomet OSSEO	677	592	160	947	440	449	200	Fracture of Implant
NB Branemark	635	501	66	806	613	695	210	Fracture of Implant
NB Replace	669	989	162	374	655	955	220	Fracture of Implant
Zimmer TSV	442	629	225	297	559	447	280	Fracture of Implant
Stmn TL	352	935	361	395	315	1102	480	Fracture of Implant

By examining the fractures of the implants, three different types could be observed. The first type was the fracture of the screw (Figure 3).

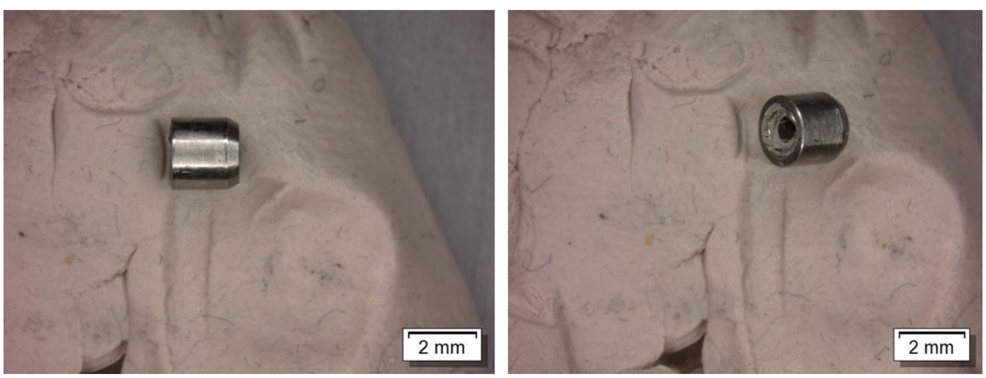

Figure 3. Fractured screw head after 908,287 cycles at 200 N load **(**Friad XIVE)

The contour plots for the σ_{max} of the implant system "Friad XIVE" which is the one with lowest maximum endured load are shown in Figure 4. The contour plots represented in this section are from the analysis with the minimum fracture force (Table 2), in order to verify the location of the failure.

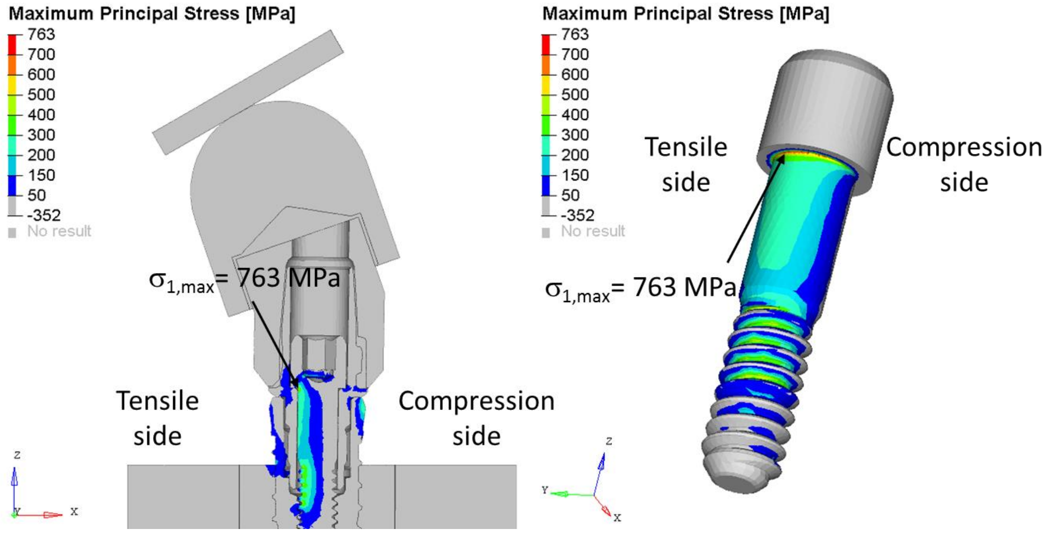

Figure 4. Distribution of the σ_{max} for the implant system Friad XIVE (left: cross section of the specimen, right: implant) for the external load of 200 N.

The second type of fracture was the fracture of the implant at the tensile side just above the embedding level. The implant systems NB Branemark, Zimmer TSV, and Biomet Osseo exhibited this kind of failure (Figure 5, Figure 7, Figure 9).

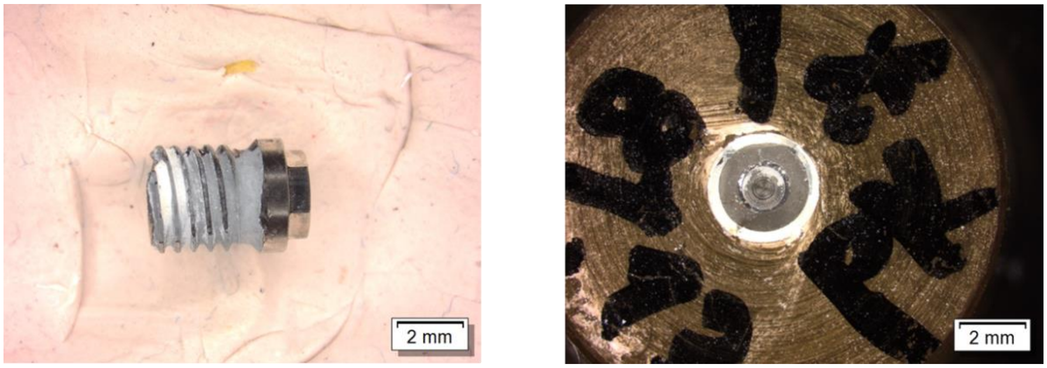

Figure 5. Fractured implant after 53,245 cycles at 250N load (NB Branemark) (left: implant, right: embedded medium with the fractured implant)

The contour plots for the σ_{max} of the implant system "NB Branemark", Biomet Osseo and Zimmer TSV are represented in Figure 6, Figure 8 and Figure 10.

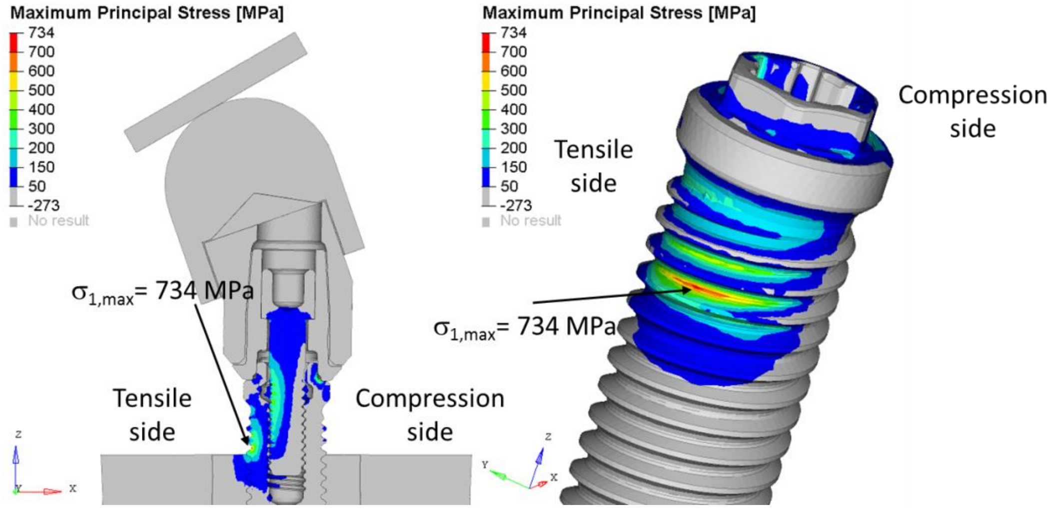

Figure 6. Distribution of the σ_{max} for the implant system NB Branemark (left: cross section of the specimen, right: implant with abutment crown) for a loading of 250N

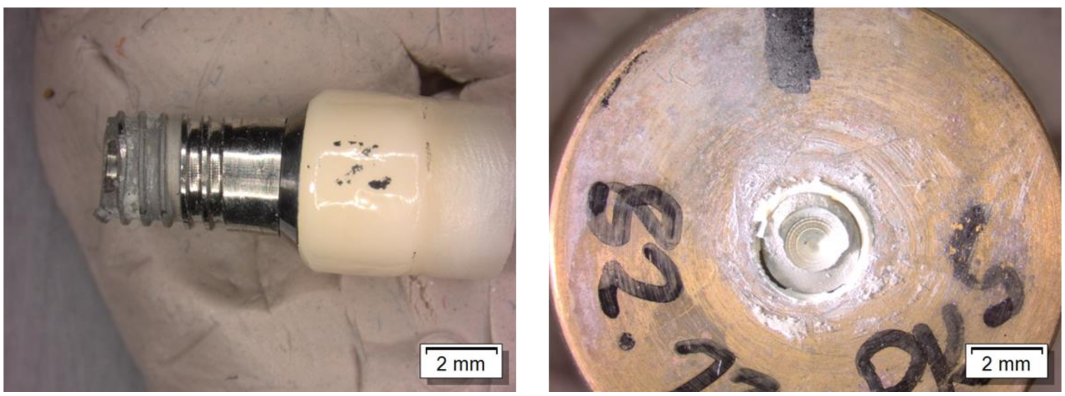

Figure 7. Fractured implant after 104650 cycles at 240N load (Biomet Osseo) (left: implant, right: embedded medium with the fractured implant)

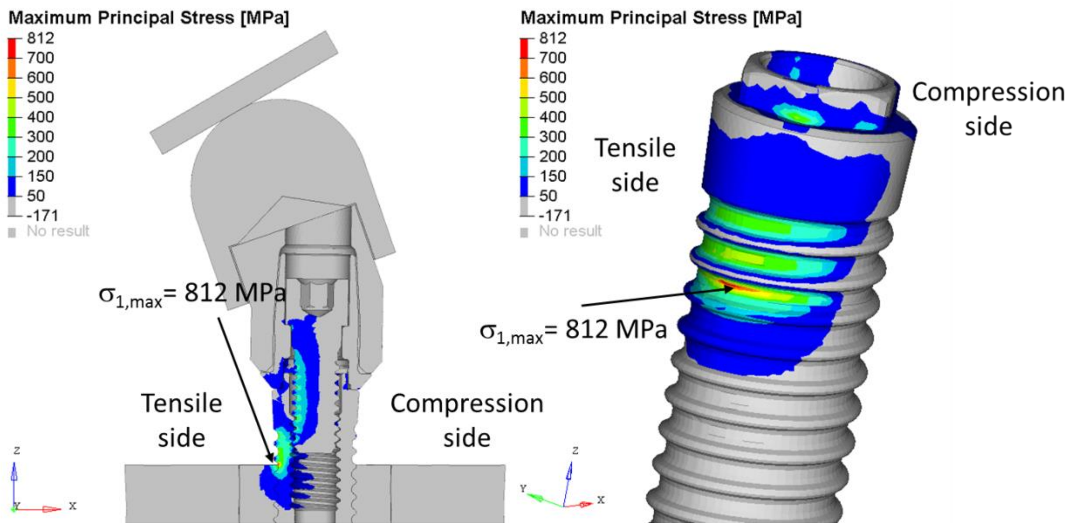

Figure 8. Distribution of the σ_{max} for the implant system Biomet Osseo (left: cross section of the specimen, right: implant with abutment crown) for the external load of 240 N.

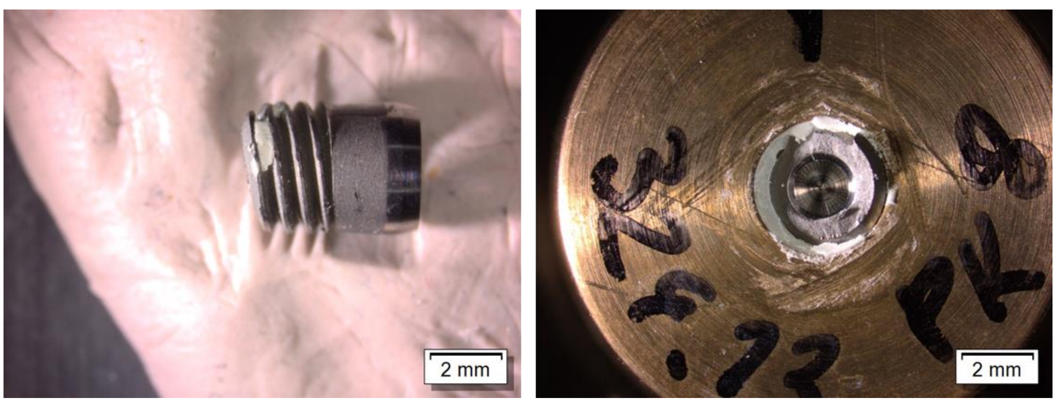

Figure 9. Fractured implant after 104031 cycles at 320 N load (Implant System Zimmer TSV) (left: implant, right: embedded medium with the fractured implant)

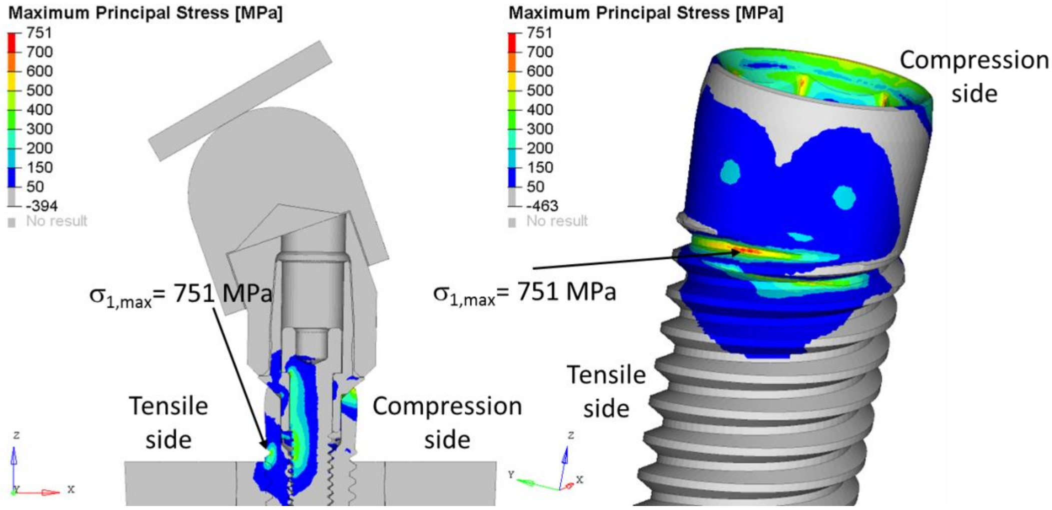

Figure 10. Distribution of the σ_{max} for the implant system Zimmer (left: cross section of the specimen, right: Implant) for the external load of 320N

The third type of fracture was the fracture of the implant head on the contact surface of the implant with abutment (NB Replace and Stmn TL, Figure 11 and Figure 13).

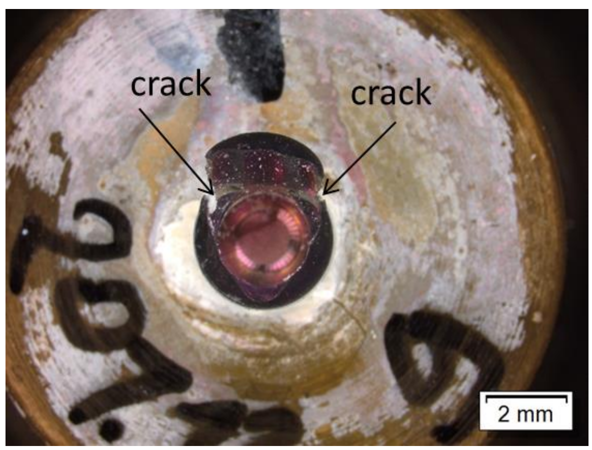

Figure 11. Fractured implant after 39,287 cycles at 280N load (NB Replace). Top view of implant with the embedded brass medium

The contour plots for the σ_{max} of the implant system NB Replace and are presented in Figure 12, Figure 14.

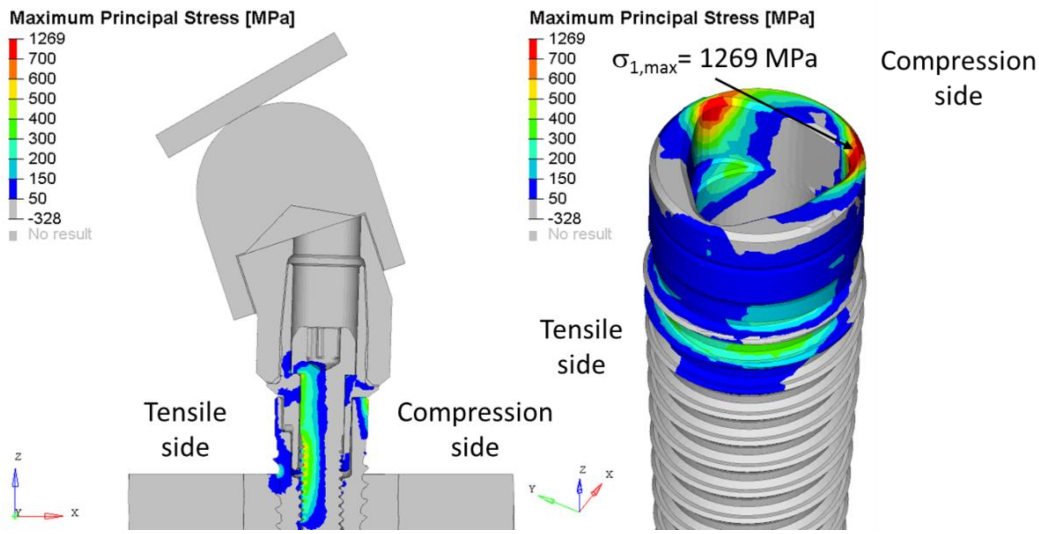

Figure 12. Fractured implant after 39,287 cycles at 280N load (NB Replace). Top view of implant with the embedded brass medium

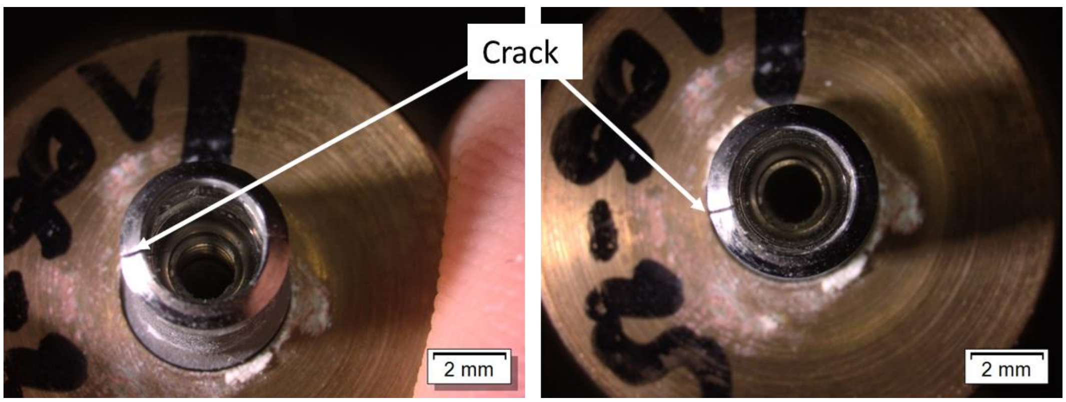

Figure 13. Fractured implant after 10501 cycles at 600 N load (Stmn TL). Top view of implant with the embedded brass medium

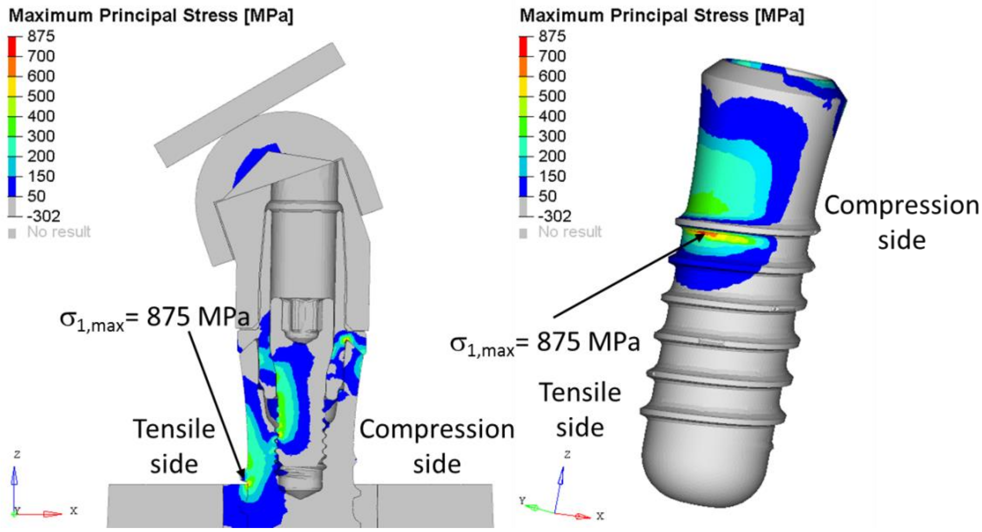

Figure 14. Distribution of the σ_{max} for the implant system Stmn TL (left: cross section of the specimen, right: Implant) for the external load of 600N

4. Discussion

The objective of this simulation study was to show the worst case implant system (with the minimum of the maximum endured load) for six different implant systems. The simulations were not aimed for making a prediction of the fatigue life of the implant systems. Accordingly, the simulations were basic FEM simulations and were only conducted for the purpose of comparing different implant systems with the aim to find out the "worst case" system.

One important simplification is that all materials considered in this investigation had been assumed to have a linear-elastic behavior. In the reality all the materials that had been considered in this investigation show a non-linear material response. The first assumption was that the plasticity of the titanium material after the yielding was not taken into account in the simulations. When examining the simulated stress values in Table 6, the stress levels of some implant systems are above the yield stress of titanium (Yield Stress Titanium Ti-6Al-4V about 940MPa, own measurements). However, the FEA simulations were conducted to define a ranking of the simulated stress values for different implant systems. Considering the plasticity may not affect this stress ranking. Secondly, adhesive materials which have a non-linear material behavior was assumed to be linear-elastic. As the adhesive layer is very thin (about 5-10 µm) [24], it was assumed that the linear-elastic response was accurate enough for this investigation and had not affected the stress of the critical components like abutment, screw and implant.

Considering the σ_{max} values simulated for the implant systems, it can be concluded that the ranking of the stress values almost matched with the ranking of the corresponding endured loads (Figure 15). The only exception was the ranking of NB Branemark and NB Replace. However, it should be noted that the NB Branemark system was only tested at 230N and 210N, and the NB Replace system was tested at 240N and 220N. Therefore, there is a chance that three NB Branemark implant/abutment specimens could have survived for a loading of 220N. For the implant system Zimmer TSV, the location of the maximum of σ_{max} matched well for the simulations with the fracture load of 320N (Figure 10). For a loading of 180N, the location of σ_{max} relocated from implant to screw (Table 6). However the value of simulated σ_{max} still correlates well for the ranking of implant systems (Figure 15). Furthermore, the simulated location of the σ_{max} matched very well with the experimental observations (Figure 3-14) except the simulations for Stmn TL implant system.

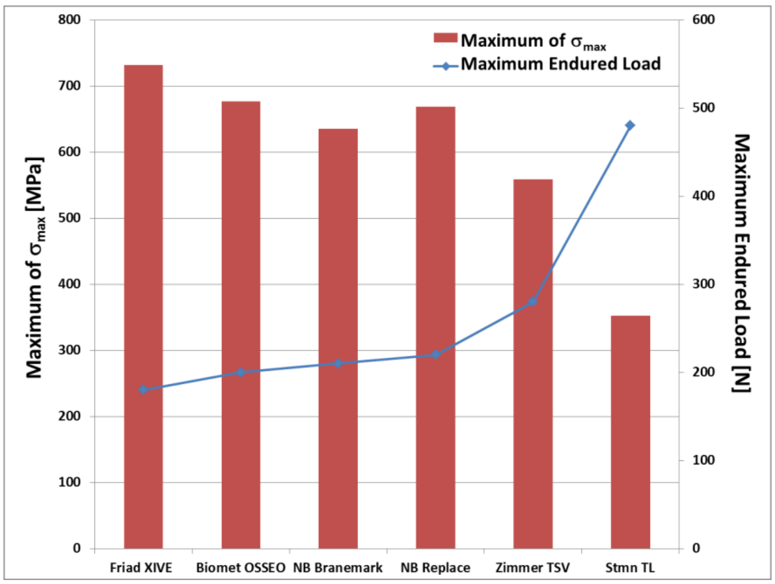

Figure 15. Maximum endured load and simulated maximum of σ_{max}

5. Conclusion and Outlook

In this investigation, a FEM simulation study was conducted to find out the worst case amongst 6 different implant systems. The "worst case" implant system for this investigation was FRIAD XIVE which has the minimum value of maximum endured load from the experiments. The simulation results were able to predict the "worst case" implant system, which has the highest maximum of σ_{max} . Furthermore the results of the FEA showed good correlation between the maximum simulated stress values and the experimental findings (Figure 15) considering the ranking of the implant systems with maximum endured load. Although the simulation results show that the simulated stresses very small for the implant system Stmn TL in comparison with the other implant systems, which matches very well the experimental results, the location of the maximum of the σ_{max} did not correlate with the location of the crack from the experiment. The experiment and the simulations for that system should be critically investigated. The linear elastic material behavior should be modified to a material model with the consideration of plasticity as the simulated stresses were above the yield strength of titanium material.

Comparing the σ_{max} values for a static loading in order to evaluate the fatigue performance of ductile materials may not be adequate. On the other hand, considering the Von-Mises values can be also quite inaccurate in order to predict the fatigue performance, as the Von-Mises stress does not give any information about the type of the stress (tensile or compressive). Furthermore comparing the result of σ_{VM} from Table 6 for the ranking of the fatigue performance of the implant systems in this study, it can be concluded that a corresponding ranking due to σ_{VM} will not correlate with the experiments.

Although the simulation results can be well verified with the experimental findings considering the σ_{max} values (which is not the case for σ_{VM}), a FEM based fatigue analysis should be carried out with programs like fe-safe, which consider the multiaxial strain state and the stress amplitude.

6. References

[1] Ivoclar Vivadent: Dental Implant & Abutment Market Report, 2016

[2] Da Silva, J.D., et al., Outcomes of implants and restorations placed in general dental practices: a retrospective study by the Practitioners Engaged in Applied Research and Learning (PEARL) Network. J Am Dent Assoc, 2014. 145(7): p. 704-13.

[3] Pjetursson, B.E., et al., I. Implant-supported FPDs. A systematic review of the survival and complication rates of fixed partial dentures (FPDs) after an observation period of at least 5 years I. Implant-supported FPDs. Clin Oral Implants Res, 2004. 15(6): p. 625-42.

[4] Lang, N.P., et al., A systematic review of the survival and complication rates of fixed partial dentures (FPDs) after an observation period of at least 5 years. II. Combined tooth--implant-supported FPDs. Clin Oral Implants Res, 2004. 15(6): p. 643-53.

[5] Creugers, N.H., et al., A systematic review of single-tooth restorations supported by implants. J Dent, 2000. 28(4): p. 209-17.

[6] Eckert SE, Meraw SJ, Cal E, Ow RK. Analysis of incidence and associated factors with fractured implants: a retrospective study. Int J Oral Maxillofac Implants, 2000, 15(5): p. 662-7.

[7] Morgan, M.J.; James, D.F.; Pilliar, R.M. Fractures of the fixture component of an osseointegrated implant.Int. J. Oral Maxillofac. Implant, 1993, 8(4): p. 409–414.

[8] Sbordone, L.; Traini, T.; Caputi, S.; Scarano, A.; Bortolaia, C.; Piattelli, A. Scanning electron microscopy fractography analysis of fractured hollow implants. J. Oral Implant. 2010, 36(2): p. 105–112.

[9] Dentistry — Implants — Dynamic loading test for endosseous dental implants 14801. Geneva, Switzerland: International Organization for Standardization; 2016.

[10] Akca K, Cehreli MC, Iplikcioglu H. Evaluation of the mechanical characteristics of the implant-abutment complex of a reduced-diameter morse taper implant. A nonlinear finite element stress analysis. Clin Oral Implants Res. 2003,14(4): p. 444-54.

[11] Geramy A, Morgano SM. Finite element analysis of three designs of an implant-supported molar crown. J Prosthet Dent, 2004, 92(5): p. 434-40.

[12] Hsu JT, Fuh LJ, Lin DJ, Shen YW, Huang HL. Bone strain and interfacial sliding analyses of platform switching and implant diameter on an immediately loaded implant: experimental and

three-dimensional finite element analyses. J Periodontol, 2009, 80(7): p.1125-32.
[13] Tepper G, Haas R, Zechner W, Krach W, Watzek G. Three-dimensional finite element analysis of implant stability in the atrophic posterior maxilla: a mathematical study of the sinus floor augmentation. Clin Oral Implants Res, 2002, 13(6): p.657-65.
[14] Şimşek B, Erkmen E, Yilmaz D, Eser A, Effects of different inter-implant distances on the stress distribution around endosseous implants in posterior mandible: A 3D finite element analysis. Medical Engineering & Physics, 2006, 28(3): p. 199-213.
[15] Eser A, Tonuk E, Akca K, Dard MM, Cehreli MC, Predicting bone remodeling around tissue- and bone-level dental implants used in reduced bone width, J of Biomechanics, 2013, 46(13): p. 2250-2257.
[16] Tsai YT, Wang KS, Woo JC, Fatigue life and reliability evaluation for dental implants based on computer simulation and limited test data. Proc. of the Institution of Mechanical Engineers, Part C: J. of Mechanical Engineering Science, 2012, 227(3): p. 554-564.
[17] Wierszycki M, Kąkol W, Łodygowski T, Fatigue Algorithm for Dental Implant. Foundations of Civil and Environmental Engineering , 2006, 7: p. 363-380.
[18] Hernandez B, Paterno A, Souza E, Freitas J, Foschini C. Fatigue analysis of dental prostheses by finite element method (FEM). International Mechanical Engineering Congress and Exposition. Houston, Texas2015.
[19] Albogha MH, Kitahara T, Todo M, Hyakutake H, Takahashi I. Maximum principal strain as a criterion for prediction of orthodontic mini-implants failure in subject-specific finite element models. Angle Orthod, 2016, 86(1): p. 24-31.
[20] Cheng YC, Lin DH, Jiang CP, Lee SY. Design improvement and dynamic finite element analysis of novel ITI dental implant under dynamic chewing loads. Biomed Mater Eng. 2015;26 Suppl 1: p. 555-61.
[21] Flanagan D, Ilies H, McCullough P, McQuoid S. Measurement of the fatigue life of mini dental implants: a pilot study. J Oral Implantol, 2008, 34(1): p. 7-11.
[22] Karl M, Kelly JR. Influence of loading frequency on implant failure under cyclic fatigue conditions. Dent Mater, 2009, 25(11): p. 1426-32
[23] Reporting of Computational Modeling Studies in Medical Device Submissions, U.S. Food and Drug Administration, 2016
[24] Albrecht T., Härdi, S., Gnos, T.: Entwicklung eines virtuellen Teststands für dentale Implantat-Abutments, KTI Report 13934.1, NTB Interstaatliche Hochschule für Technik Buchs, 2014
[25] Elgin Fastener Group, Brass, 2018, http://elginfasteners.com/resources/materials/material-specifications/brass-material/.
[26] Ivoclar Vivadent: IPS e.max CAD, Scientific Documentation, Schaan, Liechtenstein, 2011.